

ROLE OF NITROGEN ON HYDRIDE NUCLEATION IN PURE NIOBIUM BY FIRST PRINCIPLES CALCULATIONS

P. Garg, S. Balachandran, I. Adlakha, P. J. Lee, T. R. Bieler, and K. N. Solanki

Abstract

It is well known that the formation and growth of niobium hydride degrades the superconducting radio frequency (SRF) properties of niobium cavities and the treatments that reduce hydrogen concentration improve the cavity quality factor. Recently it has also been shown that the addition of nitrogen through doping or infusion improves the quality factor of SRF niobium. Thus, in this work, the role of nitrogen solute addition in niobium on hydride precipitation is probed through first-principles calculations. In the presence of nitrogen the energetic preference for hydrogen to occupy interstitial sites in the vicinity is reduced. Furthermore, both interstitial octahedral and tetrahedral sites become equally favorable for hydrogen to occupy due to the presence of nitrogen. To examine the role of nitrogen on the nucleation of hydrides, we utilized valence charge transfer and density of states calculations. These quantum insights reveal a strong tendency for nitrogen to accumulate charge, thereby decreasing the bond strength of neighboring niobium and hydrogen atoms. These atomic scale results explain the lesser tendency of surface hydride formation in SRF niobium cavities in the presence of nitrogen and are applicable to dilute Nb-H solid solutions.

INTRODUCTION

Niobium is the primary material for manufacturing superconducting radio-frequency (SRF) cavities for many modern high-performance particle accelerators like the International Linear Collider [1, 2]. The selection of superconductors for SRF applications is based on the operating temperatures (1.8 K–4.2 K) required to minimize the surface resistance and provide and sustain high electromagnetic fields in order to accelerate the charged particles inside the cavities. Niobium has the highest critical temperature (T_c) of all the pure elements (9.25 K) as well as having high critical magnetic fields and high malleability as it can be formed into complex shapes; thus, it is well suited to make SRF cavities [2]. However, niobium can readily absorb hydrogen which may occupy interstitial sites, segregate at defects or precipitate into hydride phases, depending on the hydrogen concentration and temperature, which can significantly degrade the desired properties for SRF applications [3, 4]. The performance of SRF cavities is measured in terms of the quality factor $Q_0 = G/R_s$ where the geometric factor G depends on the cavity geometry and R_s is the average surface resistance of the inner cavity wall, as a function of the accelerating gradient field (E_{acc}) [5]. Typically, niobium cavities have a Q_0 value in the range of $10^{10} - 10^{11}$ but the absorbed hydrogen contaminates niobium and severely decreases the cavity Q_0 thereby making these SRF

cavities useless [6, 7]. The formation of ordered hydride phases leads to hydrogen embrittlement and also affects the critical temperature of niobium properties since the hydride phases are not superconducting above 1-2 K [8, 9]. Therefore, improvement in the quality factor and acceleration gradients of SRF cavities is critical in the development of current and future accelerators.

Many experimental methods like X-ray, neutron and electron diffraction, differential thermal analysis (DTA), resistivity, optical microscopy, and transmission (TEM) and scanning (SEM) electron microscopy have been used to study the niobium hydrogen system for different hydrogen concentrations [7, 10–12]. Barkov *et al.* [7, 10] observed hydride precipitates of different sizes in niobium samples using laser and optical microscopy. The shape of hydride precipitates was found to be dependent on the crystallographic orientation of each grain with the presence of small hydride precipitates near the grain boundaries [7]. The diffraction patterns obtained from temperature dependent nano-area electron diffraction and scanning electron nano-area diffraction techniques further showed that Nb_4H_3 and NbH , were respectively oriented along [110] direction of Nb at cryogenic temperatures [11]. To lower surface resistance, Grassellino *et al.* [13] reported a surface treatment technique involving nitrogen doping to improve the quality factor of SRF niobium cavities. Significantly higher Q_0 values were measured for the cavity surfaces treated in nitrogen atmosphere as compared to the Q_0 values for surfaces treated with standard methods, but the underlying mechanisms are unclear [5, 13–15]. Quantitative evaluation of hydrogen in SRF cavities is difficult and in situ observations have not been possible [7, 10, 12]. The first-principles calculations showed that hydrogen absorption occurs readily into niobium [2]. Hydrogen atoms occupy interstitial tetrahedral sites, expand the crystal lattice by displacing niobium atoms from their lattice sites and create lattice distortions which decrease the structural stability of niobium [3, 16]. Furthermore, first-principles calculations also show that oxygen acts as a trapping site for hydrogen by suppressing hydrogen-hydrogen interactions and inhibiting hydride formation in niobium [17, 18]. A similar inhibiting effect is expected from nitrogen doping but the understanding is limited since such calculations have not been performed yet.

In the current work, we examine the effect of nitrogen doping on the precipitation of hydride phases in niobium through first-principles calculations. Specifically, we start by calculating the interactions between hydrogen and the niobium lattice to understand the properties of hydride phases which precipitate in niobium during service conditions. Next, we investigate the effect of nitrogen on hydrogen absorption in the niobium matrix. We find that

the presence of nitrogen reduces the energetic preference of hydrogen absorption in niobium but this effect diminishes as the distance between nitrogen and hydrogen atoms increases. The first-principles results are found to be consistent with the metallographic examination of nitrogen treated niobium coupons which show suppressed hydride concentration near the nitrogen treated surface.

COMPUTATIONAL METHODS

The first-principles calculations were performed using the Vienna ab initio simulation package (VASP) based on the density functional theory (DFT) [19, 20]. The projector augmented wave (PAW) pseudopotentials [21, 22] were utilized to represent the nuclei with valence electrons including six p electrons from the next lowest electron shell of niobium. Exchange and correlation functions were treated with the generalized gradient approximation (GGA) using the Perdew-Burke-Ernzerhof (PBE) [23] formulation. Periodic boundary conditions were used, and a plane wave basis was set with energy cutoffs of 550 eV for niobium and nitrogen and 350 eV for hydrogen. A Monkhorst-Pack k-point mesh of 12 x 12 x 12 was selected after extensive k-sampling convergence studies for geometric optimizations. The convergence studies were performed using Brillouin-zone integrations [24]. The first order Methfessel-Paxton method [25] with a smearing width of 0.2 eV was used to relax the ions with a force and energy convergence criteria of 0.01 eVÅ⁻¹ and 10⁻⁶ eV, respectively.

Interactions between hydrogen and nitrogen atoms in niobium were studied in a 2x2x2 body centered cubic (BCC) niobium unit cell with 16 niobium atoms. First, hydrogen and nitrogen atoms were added at interstitial sites in a niobium supercell, corresponding to Nb₁₆H₁ and Nb₁₆N₁, respectively, in order to understand the interactions between hydrogen and niobium atoms and nitrogen and niobium atoms, respectively. Next, a hydrogen atom was doped at different interstitial sites while keeping the nitrogen atom at an octahedral site in niobium to examine the co-segregation behavior of hydrogen and nitrogen with the niobium lattice. Electronic density of states (DOS) and valence charge transfer calculations were also performed for different structures to understand the changes that occur in bonding between different atoms. DOS curves describe the number of states per interval of energy at each energy level that are available to be occupied [26]. To obtain valence charge transfer which takes place upon addition of different solute atoms, ground state non-interacting charge densities were

subtracted from the valence charge density of the interacting system. Hence, the valence charge transfer was calculated as:

$$\Delta\rho = \rho_{\text{Nb-H-N}} - \rho_{\text{Nb}} - \rho_{\text{H}} - \rho_{\text{N}} \quad (1)$$

where $\Delta\rho$ represents the total valence charge transfer, $\rho_{\text{Nb-H-N}}$ represents the valence charge density of the interacting Nb-H-N system, and ρ_{Nb} , ρ_{H} and ρ_{N} , respectively, represent the valence charge density of non-interacting and isolated niobium, hydrogen and nitrogen atoms. The VESTA (visualization for electronic and structural analysis) software package [27] was utilized to extract the valence charge transfer contours from the first-principles calculations.

RESULTS AND DISCUSSION

The calculated lattice parameter of 3.32 Å for BCC niobium is in good agreement with experimentally and theoretically reported values [2, 3]. In pure niobium, absorption of both hydrogen in tetrahedral sites and nitrogen in octahedral sites is energetically favorable, releasing 0.28 eV and 1.98 eV, respectively. The DOS curve of Nb₁₆H₁ had a peak at -7 eV which was absent in the DOS pattern of pure niobium (see Figure 1a). This peak corresponds to the overlap of the *1s* state of hydrogen with *s* and *d* states of niobium indicating the possibility of covalent bonding between niobium and interstitial hydrogen atoms. Similarly, the peak at -6 eV in the DOS curve of Nb₁₆N₁, due to the overlap of *2p* states of nitrogen with *d* states of niobium, indicates possible covalent bonding between niobium and nitrogen (see Figure 1b). The peak at -15 eV in Nb₁₆N₁ corresponds to the *s* orbital electrons of nitrogen. From the valence charge transfer calculations, we see that charge is accumulated (yellow iso-surface) around interstitial hydrogen or nitrogen atoms respectively and depleted (cyan iso-surface) from the surrounding niobium atoms (see Figure 1c and 1d). Thus, both the solute atoms have partially anionic character in niobium since charge is accumulated around each solute atom. Nitrogen also has a stronger anionic character than hydrogen since the charge redistribution in niobium is much greater upon nitrogen addition. Valence charge transfer contours are plotted at an iso-surface value of 0.027e/Å³. Niobium atoms are represented by dark grey spheres while the hydrogen atom is represented by an orange sphere and the nitrogen atom is represented by a blue sphere (below the iso-surface).

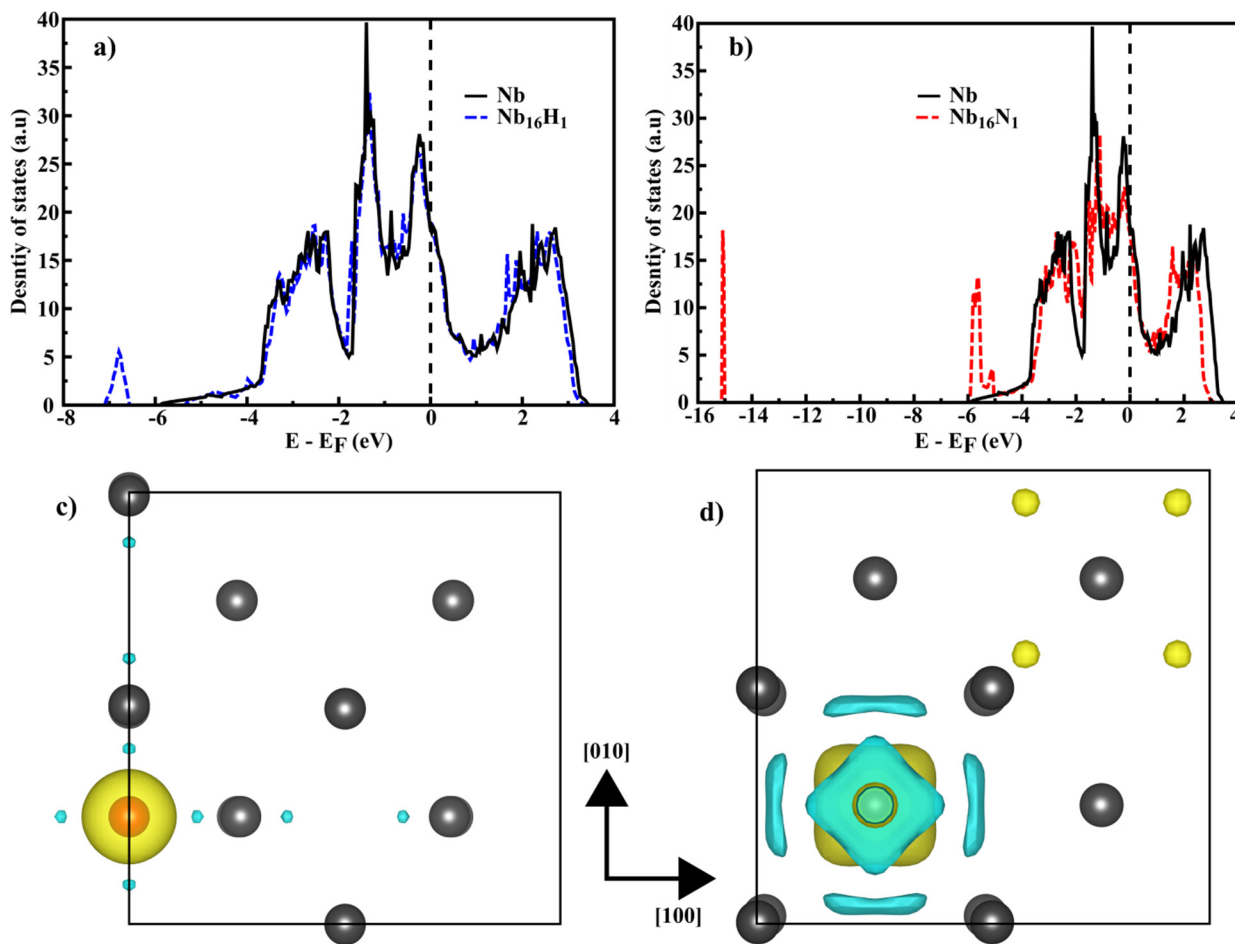


Figure 1: Total density of state patterns for (a) $Nb_{16}H_1$ (hydrogen atom at a tetrahedral site) and (b) $Nb_{16}N_1$ (nitrogen atom at an octahedral site), respectively. The valence charge density transfer contours for (c) $Nb_{16}H_1$ and (d) $Nb_{16}N_1$, respectively. Yellow and cyan iso-surfaces respectively represent charge accumulation and depletion at a value of $0.027 \text{ e}/\text{\AA}^3$ in (c) and (d).

Next, we calculated the energy changes that occurred upon absorption of a hydrogen atom at different interstitial sites in the presence of a nitrogen atom at an octahedral site in niobium. The nitrogen atom at an octahedral site significantly affects the energetics of hydrogen absorption in niobium since the interstitial sites in the vicinity of nitrogen are no longer energetically favorable for hydrogen absorption. Hydrogen absorption becomes an endothermic process (positive formation energy values) at interstitial sites up to $\sim 2\text{\AA}$ away from nitrogen (see Figure 2). The suppression effect of nitrogen diminishes on interstitial sites farther away as the formation energy reduces to zero and finally becomes negative. Interestingly, it was seen that both tetrahedral and octahedral sites, farther away from nitrogen, have similar favorability for hydrogen absorption since the energy released is similar at both the sites (see Figure 2).

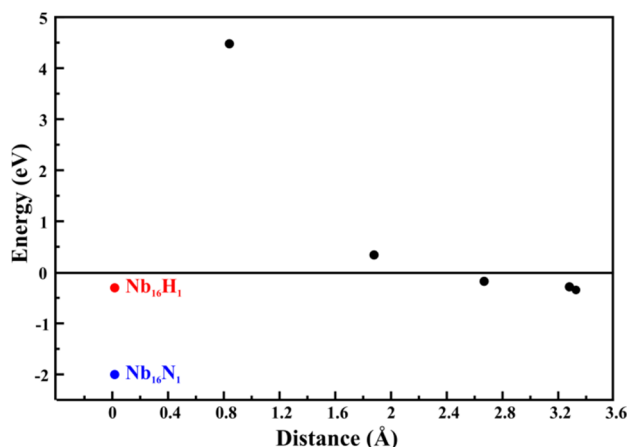


Figure 2: Reference energies for a nitrogen atom at an octahedral site (blue) and a hydrogen atom at a tetrahedral site (red) are shown at position 0. The binding energy of a hydrogen atom is higher than the reference value when it is closer than 3\AA from a N atom.

The observed changes in energy can be understood through electronic DOS and valence charge transfer calculations. The peak at -7 eV in the DOS curves in Figure 3 corresponds to the overlap of states of hydrogen with

Content from this work may be used under the terms of the CC BY 3.0 licence (© 2017). Any distribution of this work must maintain attribution to the author(s), title of the work, publisher, and DOI.

states of niobium irrespective of the hydrogen atom occupying either a tetrahedral (T) or octahedral (O) site far away from nitrogen. The peak at -6 eV is due to the overlap of $2p$ states of nitrogen with d states of niobium. Thus, a nitrogen atom located far away from hydrogen does not interfere in the covalent bonding between hydrogen and niobium atoms. The valence charge transfer contours are also very similar in both cases of a hydrogen atom

occupying either a T or O site since the charge depleted (cyan iso-surface) from the niobium atoms is accumulated (yellow iso-surface) around hydrogen and nitrogen atoms respectively. Thus, we see that nitrogen suppresses hydrogen absorption in niobium, but the suppressing effect diminishes at interstitial sites located far away from the nitrogen atom.

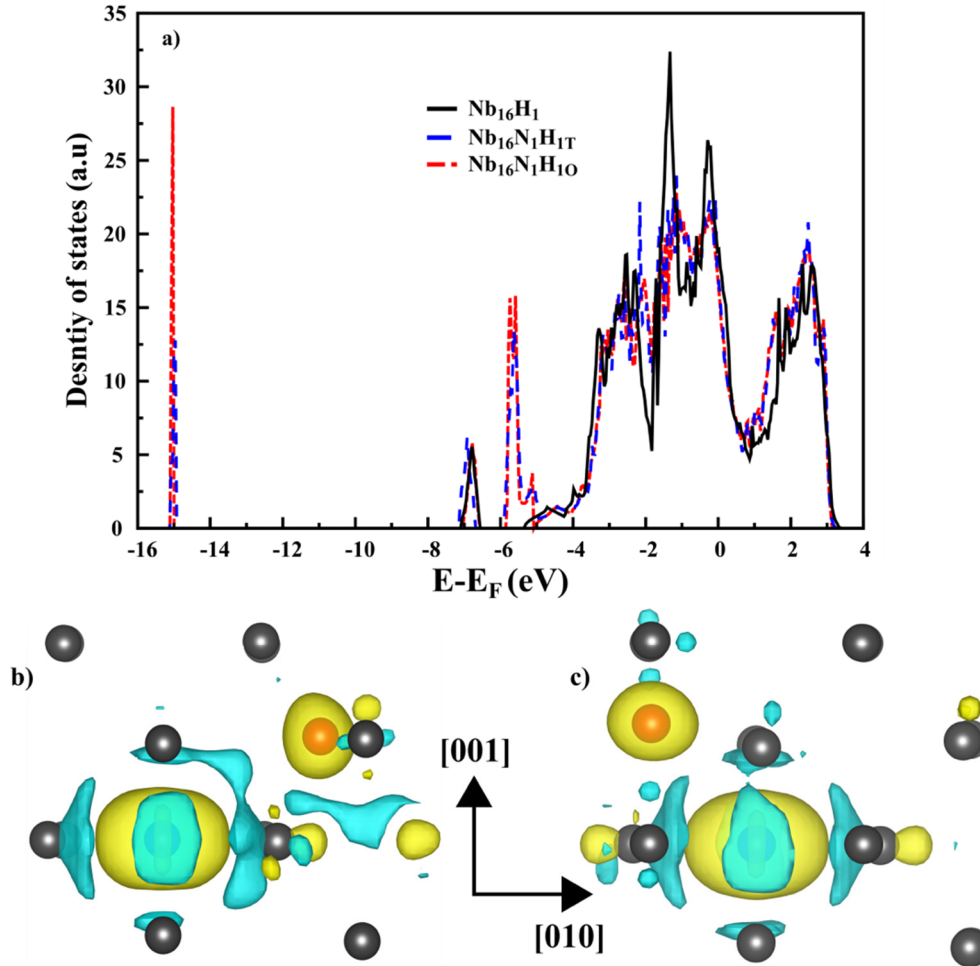


Figure 3: (a) Electronic DOS patterns for $Nb_{16}H_1$ compared to the DOS pattern of $Nb_{16}N_1$ with a hydrogen atom absorbed at different interstitial sites far away from nitrogen. The valence charge transfer plots for $Nb_{16}N_1$ with a hydrogen atom absorbed at (b) a tetrahedral (T) site and (c) an octahedral (O) site, respectively. Yellow and cyan iso-surfaces respectively represent charge accumulation and depletion with a value $0.027e/A^3$ in (b) and (c).

CONCLUSIONS

First-principles calculations show that nitrogen doping suppresses hydrogen absorption in niobium. The suppressing effect of nitrogen is dominant in its vicinity as indicated by the positive value of formation energy. But, hydrogen absorption becomes favorable at both tetrahedral and octahedral interstitial sites away from nitrogen as the formation energy becomes negative. The DOS patterns and valence charge transfer calculations explain that nitrogen doping affects the bonding between hydrogen and niobium atoms which diminishes hydrogen absorption in niobium.

REFERENCES

- [1] Z.-H. Sung *et al.*, “Development of low angle grain boundaries in lightly deformed superconducting niobium and their influence on hydride distribution and flux perturbation”, *J. Appl. Phys.*, vol. 121, p. 193903, 2017.
- [2] D. C. Ford, L. D. Cooley, D. N. Seidman, “First-principles calculations of niobium hydride formation in superconducting radio-frequency cavities”, *Supercond. Sci. Technol.*, vol. 26, p. 095002, 2013.
- [3] G. Alefeld, J. Völkl, “Hydrogen in metals I-Basic properties”, *Berlin and New York, Springer-Verlag (Topics in Applied Physics)*, vol. 28, p. 442, 1978.
- [4] R. Tao, A. Romanenko, L. D. Cooley, R. F. Klie, “Low temperature study of structural phase transitions in niobium hydrides”, *J. Appl. Phys.*, vol. 114, p. 044306, 2013.

- [5] P. Dhakal, G. Ciovati, P. Kneisel, G. R. Myneni, "Enhancement in Quality Factor of SRF Niobium Cavities by Material Diffusion", *IEEE Trans. Appl. Supercond.*, vol. 25, pp. 1–4, 2015.
- [6] J. Knobloch, (AIP, 2003; <http://aip.scitation.org/doi/abs/10.1063/1.1597364>), vol. 671, pp. 133–150.
- [7] F. Barkov, A. Romanenko, Y. Trenikhina, A. Grassellino, "Precipitation of hydrides in high purity niobium after different treatments", *J. Appl. Phys.*, vol. 114, p. 164904, 2013.
- [8] N. M. Jisrawi *et al.*, "Reversible depression in the Tc of thin Nb films due to enhanced hydrogen adsorption", *Phys. Rev. B.*, vol. 58, p. 6585, 1998.
- [9] S. Isagawa, "Hydrogen absorption and its effect on low-temperature electric properties of niobium", *J. Appl. Phys.*, vol. 51, pp. 4460–4470, 1980.
- [10] F. Barkov, A. Romanenko, A. Grassellino, "Direct observation of hydrides formation in cavity-grade niobium", *Phys. Rev. Spec. Top. Accel. Beams*, vol. 15, 2012, doi:10.1103/PhysRevSTAB.15.122001.
- [11] Y. Trenikhina, A. Romanenko, J. Kwon, J.-M. Zuo, J. F. Zasadzinski, "Nanostructural features degrading the performance of superconducting radio frequency niobium cavities revealed by transmission electron microscopy and electron energy loss spectroscopy", *J. Appl. Phys.*, vol. 117, p. 154507, 2015.
- [12] T. Schober, M. A. Pick, H. Wenzl, "Electron microscopy of β -hydride in niobium", *Phys. Status Solidi A.*, vol. 18, pp. 175–182, 1973.
- [13] A. Grassellino and A. Romanenko and D. Sergatskov and O. Melnychuk and Y. Trenikhina and A. Crawford and A. Rowe and M. Wong and T. Khabiboulline and F. Barkov, "Nitrogen and argon doping of niobium for superconducting radio frequency cavities: a pathway to highly efficient accelerating structures", *Supercond. Sci. Technol.*, vol. 26, p. 102001, 2013.
- [14] D. Gonnella, M. Liepe, "New insights into heat treatment of SRF cavities in a low-pressure nitrogen atmosphere", *Proc. IPAC'14*, pp.2634–2637, 2014.
- [15] D. Gonnella, M. Ge, F. Furuta, M. Liepe, "Nitrogen treated cavity testing at Cornell", *Proceedings of LINAC*. 2014.
- [16] P. Khowash, S. Gowtham, R. Pandey, "Electronic structure calculations of substitutional and interstitial hydrogen in Nb", *Solid State Commun.*, vol. 152, pp. 788–790, 2012.
- [17] D. C. Ford, L. D. Cooley, D. N. Seidman, "Suppression of hydride precipitates in niobium superconducting radio-frequency cavities", *Supercond. Sci. Technol.*, vol. 26, p. 105003, 2013.
- [18] D. C. Ford, P. Zapol, L. D. Cooley, "First-Principles Study of Carbon and Vacancy Structures in Niobium", *J. Phys. Chem. C.*, vol.119, pp. 14728–14736, 2015.
- [19] G. Kresse, J. Hafner, "Ab initio molecular dynamics for liquid metals", *Phys. Rev. B.*, vol. 47, p. 558, 1993.
- [20] G. Kresse, J. Hafner, "Norm-conserving and ultrasoft pseudopotentials for first-row and transition elements", *J. Phys. Condens. Matter.*, vol. 6, p. 8245, 1994.
- [21] P. E. Blöchl, O. Jepsen, O. K. Andersen, "Improved tetrahedron method for Brillouin-zone integrations", *Phys. Rev. B.*, vol.49, p. 16223, 1994.
- [22] G. Kresse, J. Furthmüller, "Efficient iterative schemes for ab initio total-energy calculations using a plane-wave basis set", *Phys. Rev. B.*, vol.54, p. 11169, 1996.
- [23] P. E. Blöchl, Projector augmented-wave method. *Phys. Rev. B.*, vol.50, p. 17953, 1994.
- [24] H. J. Monkhorst, J. D. Pack, "Special points for Brillouin-zone integrations", *Phys Rev B.*, vol. 13, p. 5188–5192, 1976.
- [25] P. Pulay, "Convergence acceleration of iterative sequences. The case of SCF iteration", *Chem. Phys. Lett.*, vol. 73, pp. 393–398, 1980.
- [26] M. E. Pronsato, C. Pistonesi, A. Juan, "Density functional study of H-Fe vacancy interaction in bcc iron", *J. Phys. Condens. Matter.*, vol.16, pp. 6907–6916, 2004.
- [27] K. Momma, F. Izumi, "VESTA: a three-dimensional visualization system for electronic and structural analysis", *J. Appl. Crystallogr.*, vol. 41, pp. 653–658, 2008.